Article

Journal of Vibration and Control
2023, Vol. 29(13-14) 3038–3051

DOI: 10.1177/10775463221090325
journals.sagepub.com/home/jvc
Sage

Optimization of structural design with pendulum dynamic vibration absorber using genetic algorithm

Hoo Min Lee[1], Sol Ji Han[1], Deok-Soo Kim[1], and Gil Ho Yoon[1]

Abstract

In this study, a genetic algorithm is introduced to determine optimal locations of pendulum dynamic vibration absorbers (PDVAs) in vibrating structures. A PDVA is composed of a pendulum system and spring-mass system, and aims to attenuate structural vibrations at two resonance frequencies, that is, the square root of stiffness over mass and square root of a length over gravity of the hosting structure. An optimization method involving nonlinear transient finite element analysis was applied to increase the engineering efficiency of PDVAs. With the incorporation of a genetic algorithm, the optimal locations of PDVAs in various structures can be determined and vibrations at the desired resonant frequencies can be attenuated. In addition, the Voronoi diagram concept is applied to realize a uniform distribution of PDVAs in vibrating structures. Several optimization examples were solved using the proposed genetic algorithm and demonstrated decreases in frequency responses by up to 98.6549%, showing the effectiveness of PDVAs in suppressing structural vibrations.

Keywords

pendulum dynamic vibration absorber, genetic algorithm, lattice structure, vibration suppression, Voronoi diagram

1. Introduction

The present study aims to achieve structural stability through vibration suppression. Therefore, a pendulum dynamic vibration absorber (PDVA) was used to attenuate the vibrations in various structures. Pendulum dynamic vibration absorbers are installed on finite element nodes and junctions of lattice structures. A genetic algorithm (GA) was used to determine the optimal locations of PDVAs in the hosting structures to establish optimal structural designs with vibrations suppressed at the desired resonant frequencies. The Voronoi diagram was applied to realize a uniform distribution of PDVAs. Several numerical examples were solved to validate the proposed method.

Structural instability arising from various vibrational motions is an important subject in the engineering field. Many studies have been conducted on the effect of vibrations on the instability of carbon nanotubes (Yoon et al., 2005), vibration fatigue in aerospace structures (Aykan and Celik 2009), transient vibration of unit-plant structures (Zhang et al., 2019), structural vibration of wind turbine structures (Dong et al., 2018), and vibration characteristics of high-speed railway structures (Jiang et al., 2019) to analyze the structural instabilities arising from external forces. Moreover, some studies have explored various factors affecting the vibration characteristics. To this end, force harmonics and their effects on vibration (Zou et al., 2017), relationships between cutting parameters and vibration (Chuangwen et al., 2018), effect of multidimensional forces on vibration suppression (Zhao et al., 2021), and effect of periodic fluid forces on the vibration of tube bundles (Lai et al., 2021) have been analyzed to explore the effect of various forces on vibration characteristics. In addition, many studies have been directed on the presence of acoustic black holes for vibration control (Zhao and Prasad 2019), optimum design of DC motors for vibration reduction (Jafarboland and Farahabadi 2018), effect of the volume fraction of carbon nanotubes on damping properties (Patnaik et al., 2021), vibration characteristics of plates with viscoelastic periodic cores (Sheng et al., 2018), lattice structures (Syam et al., 2018), and sandwich structures with rotating carbon nanotubes (Hussain et al., 2019) to explore

[1]Department of Mechanical Engineering, College of Engineering, Hanyang University, Seoul, Korea

Received: 5 October 2021; revised: 21 February 2022; accepted: 10 March 2022

Corresponding author:
Gil Ho Yoon, Department of Mechanical Engineering, College of Engineering, Hanyang University, Seoul 04763, Korea.
Email: gilho.yoon@gmail.com

the effect of structural designs on vibration behaviors. Free vibration analysis of porous functionally graded nanoplates (Phung-Van et al., 2019), test evaluation of the vibration reduction effect of stone mastic asphalt mixture (Luo et al., 2021), analysis of the effect of porosity on the vibration characteristics of composite structures (Pourjabari et al., 2019), and finite element analysis (FEA) of natural fiber-reinforced composites (Saini et al., 2021) have been performed to investigate the influence of material composition on vibration behaviors. Furthermore, many studies have been conducted to develop a nonlocal couple stress theory (Ebrahimi et al., 2020), investigate the structural behavior of plates on an elastic foundation (Kaddari et al., 2020), analyze nanobeams including thermal effects (Hamza-Cherif et al., 2018), analyze shear-deformable tapered beams (Ghayesh 2018), develop a size-dependent sinusoidal beam model (Lu et al., 2017), analyze plates using nonlocal trigonometric shear deformation theory (Besseghier et al., 2017), and present a Fourier series solution for vibration analysis (Qin et al., 2020). Despite the uncertainties that lead to structural instabilities, the vibration phenomenon has been intentionally used in engineering fields for various purposes. Vibration energy harvesting methods (Abdelkareem et al., 2018; Wu et al., 2018; Zhao and Yang 2018) and vibration-based crack identification methods (Prawin and Rama Mohan Rao 2020; Jena 2018) have been developed and utilized in recent years. An increasing demand for vibration applications in various fields has increased the need to control the vibration phenomena. Moreover, various methods have been introduced to control and attenuate vibrations. Methods using metamaterials (Meng et al., 2020; Elmadih et al., 2019) and thickening fluids (Gürgen and Sofuolu 2020) have been developed to achieve vibration attenuation. Vibration suppression methods have been successfully applied to multi-story building structures (Chapain and Aly 2019) and wing systems (He et al., 2020). Therefore, suppressing and controlling vibrations within structures have been reported frequently. However, these studies have revealed limitations to some extent, where vibration is suppressed only at certain frequency ranges or directions. It is an important issue in the engineering field to suppress vibrations at resonant frequencies regardless of vibration direction, as vibrational motions at those frequencies are critical in causing structural instability. Thus, we aimed to develop a system using dynamic vibration absorbers to focus on the reduction of vibration responses at several targeted frequency ranges, regardless of the vibration direction. Dynamic vibration absorber functions by separating and shifting the eigen-frequencies of the hosting structure, and reduces the responses at target frequencies (Kalehsar and Khodaie 2018). Though increase in responses at neutral frequency ranges not responsible for structural instability can be induced, the application of dynamic vibration absorbers results in the achievement of overall structural stability (Krenk 2005). The proposed method utilizes the PDVA which has been numerically and experimentally verified in suppressing vibrations at multiple frequency ranges (Ha and Yoon 2021). The system can be applied to beam, lattice, and plane structures for suppression of vibration at multiple frequency ranges and directions simultaneously, as we validated its application in real-world engineering considering a variety of structure types.

The proposed PDVA system attenuates vibrations in structures by tuning the eigen-frequencies of the pendulum and spring-mass systems, whereas the performance of vibration suppression can be changed by varying the locations of PDVAs in a structure. Thus, we determined the optimum locations of PDVAs installed in structures with vibrating motions. In the proposed optimization method, the integer design variables, indicating the node numbers of the finite element models of the structures, were set as the design variables. For the optimization method, evolutionary algorithms and nature inspired methods were considered due to their robustness and flexibility to capture global solutions of complex optimization problems (Galvan et al., 2003). Among the various optimization methods capable of finding the global optimum, such as particle swarm optimization (Couceiro and Ghamisi 2016; Chopard and Tomassini 2018) and differential evolution (Qin et al., 2008; Das et al., 2013), GA was chosen, the reason being that GA is more suitable for discrete optimization problems (Kachitvichyanukul 2012). The GA was used to obtain the optimum installation locations by employing the real coded GA implemented in the MATLAB software package. Additionally, nonlinear transient FEA was performed to evaluate the vibration suppression performance of PDVAs. The concept of the Voronoi diagram was employed to uniformly distribute PDVAs in a structure to prevent PDVAs from being focused on a certain domain of a structure. The Voronoi diagram divides the hosting structures into several sub-domains, and PDVAs are uniformly distributed by limiting the number of PDVAs in each sub-domain. The mapping approach was employed to accurately locate PDVAs at each sub-domain of structures. With the proposed optimization method, optimal structural designs can be acquired using PDVAs. Several case studies were analyzed using the proposed framework to validate its efficiency and accuracy.

The remainder of this paper is organized as follows. Section 2 describes the theory of the PDVA mechanism using FEA. In Section 3, optimization formulations for the GA and Voronoi diagram concept are presented. Section 4 provides several structural optimization examples considering the installation of PDVAs. Finally, Section 5 draws the conclusions and discusses the future study directions.

1.1 Pendulum dynamic vibration absorber

Here, the PDVA mechanism theory is developed using FEA. To simulate the vibrations of structures with and

without PDVA allowing nonlinear vibration motion, transient analyses were conducted in the ANSYS framework, and frequency response functions of transient responses were analyzed.

1.2 Equations of motion

Figure 1 demonstrates a schematic of PDVA, which utilizes the resonances of the pendulum and spring-mass systems, with a concentrated mass m_p, spring with a length l_0 and spring constant k_p, and a damper with damping constant c_p. A common vibration absorber utilizes only one of the radial and vertical motions. However, PDVAs utilize both motions simultaneously for vibration attenuation. Moreover, PDVAs are excited both vertically and horizontally, even when the hosting structure moves only horizontally. By tuning the eigen-frequencies of the pendulum to external vibration frequencies, the hosting structure vibration can be effectively attenuated. Additionally, the governing equations of the system can be simplified by the linear rotation assumption; however, the proposed PDVA system performs a transient nonlinear analysis on the frequency response function. The governing equations of the PDVA system were defined using the Lagrange approach. The kinetic energy T of the PDVA system can be defined as follows

$$\begin{aligned} T &= \frac{1}{2}m\dot{x}_1^2 + \frac{1}{2}m_p a \\ a &= \dot{x}_1^2 + b^2\dot{\theta}^2 + \dot{u}^2 + 2\dot{x}_1\dot{\theta}b\cos\theta + 2\dot{u}\dot{x}_1\sin\theta \\ b &= l_0 + u \end{aligned} \tag{1}$$

where m and $\dot{x}_1$ denote the mass and velocity of the hosting structure, respectively. m_p and l_0 denote the mass of the pendulum and length of the spring in the PDVA system, respectively. u, $\dot{u}$, θ, and $\dot{\theta}$ represent the displacement, velocity, angular displacement, and angular velocity of PDVA, respectively. As both the rotational and translational motions of the pendulum mass should be considered, the velocity term associated with the rotation, $\dot{\theta}$, is used. The potential energy V of the PDVA system can be defined using the rotation of pendulum as follows

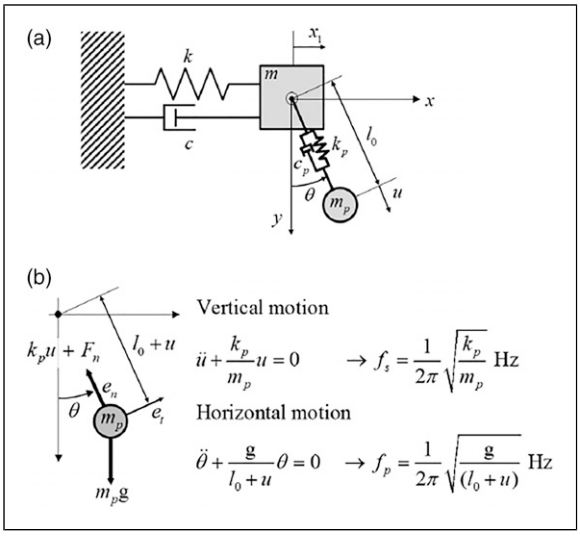

Figure 1. (a) Illustration of PDVA and (b) mechanism of PDVA.

$$V = \frac{1}{2}kx_1^2 + \frac{1}{2}k_p u^2 + m_p g b(1-\cos\theta) \tag{2}$$

where k and x_1 represent the spring constant and displacement of the hosting structure, respectively. k_p and g represent the spring constant of the PDVA system and gravitational acceleration, respectively. The energy dissipation F owing to damping is defined as follows

$$F = \frac{c\dot{x}_1^2}{2} + \frac{c_p\dot{u}^2}{2} \tag{3}$$

where c and c_p denote the damping constants of the hosting structure and PDVA system, respectively. The Lagrangian approach can be applied to the governing equation

$$\mathbf{A}_1 = \begin{bmatrix} m+m_p & m_p b\cos\theta & m_p\sin\theta \\ m_p b\cos\theta & m_p b^2 & 0 \\ m_p\sin\theta & 0 & m_p \end{bmatrix} \begin{bmatrix} \ddot{x}_1 \\ \ddot{\theta} \\ \ddot{u} \end{bmatrix} \tag{4}$$

$$\mathbf{A}_2 = \begin{bmatrix} c & 0 & 0 \\ 0 & 0 & 0 \\ 0 & 0 & c_p \end{bmatrix} \begin{bmatrix} \dot{x}_1 \\ \dot{\theta} \\ \dot{u} \end{bmatrix} \tag{5}$$

$$\mathbf{A}_3 = \begin{bmatrix} k & 0 & 0 \\ 0 & 0 & 0 \\ 0 & 0 & k_p \end{bmatrix} \begin{bmatrix} x_1 \\ \theta \\ u \end{bmatrix} \tag{6}$$

$$\mathbf{A}_4 = \begin{bmatrix} -m_p b\dot{\theta}^2\sin\theta + 2m_p\dot{u}\dot{\theta}\cos\theta \\ 2m_p b\dot{u}\dot{\theta} + m_p g b\sin\theta \\ -m_p b\dot{\theta}^2 + m_p g(1-\cos\theta) \end{bmatrix} \tag{7}$$

$$\mathbf{A}_1 + \mathbf{A}_2 + \mathbf{A}_3 + \mathbf{A}_4 = \mathbf{0} \tag{8}$$

In equation (4), $\ddot{x}_1$, $\ddot{\theta}$, and $\ddot{u}$ denote the acceleration of the hosting structure, angular acceleration of PDVA, and acceleration of PDVA, respectively. The vertical and horizontal motions of PDVA were defined using the Lagrangian approach, as shown in Figure 1(b). The figure also shows the mechanism of the PDVA, where the resonant frequencies of the spring-mass system and the

pendulum system are affected by different parameters. The spring-mass system takes part in the PDVA's vertical motion, and the system's resonant frequency value changes when the pendulum mass and the spring constant of the PDVA are modified. The pendulum system takes part in the PDVA's horizontal motion, and the system's resonant frequency value changes when the pendulum length of the PDVA is modified. As the parameters affecting the resonant frequencies of the pendulum and spring-mass systems of PDVAs are different, the two resonant frequencies can be independently tuned, to be utilized regardless of the direction of vibration in a vibrating structure.

1.3 Nonlinear transient finite element simulation of PDVA system

Computing the frequency response function of a PDVA system is challenging owing to the transient nonlinearity of the governing equations. We employed a transient nonlinear finite element simulation (time discretization using the Newmark scheme in ANSYS) to obtain nonlinear responses. The dependency of the internal force, $\mathbf{F^i}$, with respect to the transient displacement vector, $\mathbf{U}$, becomes the origin of the nonlinearity.

$$\mathbf{M}\ddot{\mathbf{U}}(t) + \mathbf{C}\dot{\mathbf{U}}(t) + \mathbf{F}^i(\mathbf{U},t) = \mathbf{F}^a(t) \tag{9}$$

Here, $\mathbf{M}$ and $\mathbf{C}$ represent the mass and damping matrices, respectively; $\mathbf{F}^i(t)$ and $\mathbf{F}^a(t)$ denote the internal and external forces, respectively. As the internal force is formulated using the theory of a nonlinear PDVA system, it depends on the displacement vector $\mathbf{U}$. The velocity and acceleration vectors are denoted by $\dot{\mathbf{U}}$ and $\ddot{\mathbf{U}}$, respectively. Nonlinear equations are typically solved after linearization. The above nonlinear equations should be solved iteratively to analyze the motion of PDVA while admitting finite rotation.

An example considering a hosting beam structure was solved to demonstrate the applicability of the proposed method. Figure 2 shows the problem definition and obtained results. A straight hosting structure consisting of five frame elements was considered. The frame structure was set to have a Young's modulus of 193 GPa, Poisson's ratio of 0.31, and density of 7750 kg/m^3. The width and height of the frame's cross-section was 0.10 and 0.05 m, respectively. A mass of 20 kg and impact forces of 1000 N in the y- and z-direction were applied at the end of the structure. PDVA, with a mass of 10 kg, length of 0.0151 m, and spring constant of 9.305×10^4 N/m, was also installed at the end of the structure. The pendulum resonance frequency was 4.101 Hz, considering the installed PDVA. The vibration attenuation performance of the PDVA can be seen from the two graphs in Figure 2. From the frequency response function (FRF) graph, it can be observed that the displacement amplitude at 4.101 Hz has decreased, indicating

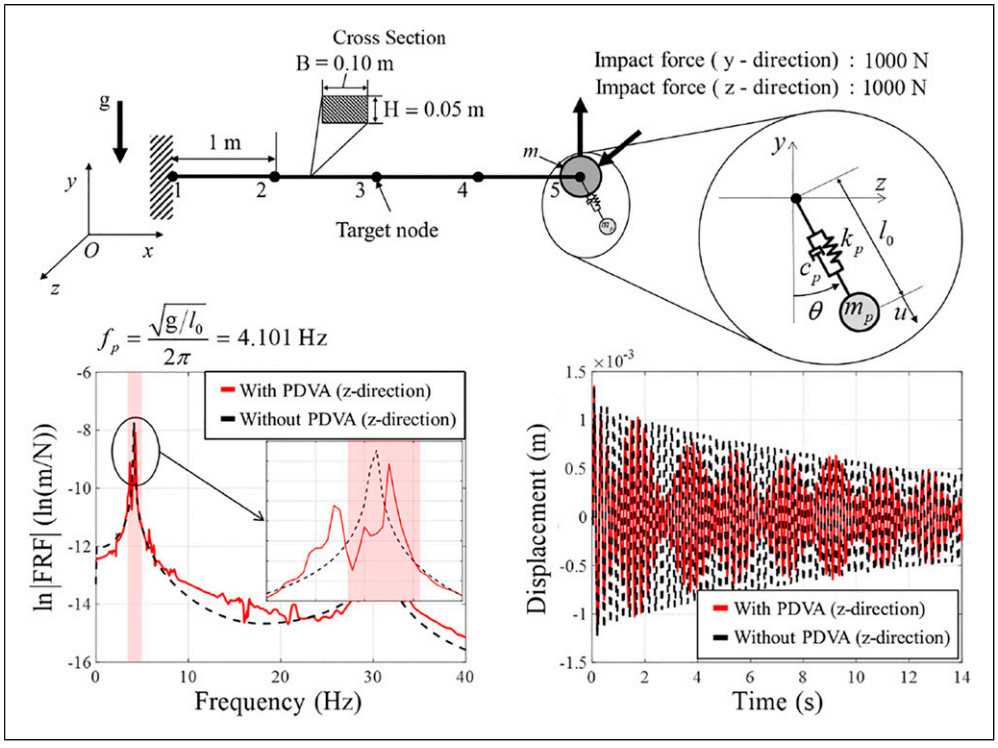

Figure 2. Example of PDVA attached to a 5-m hosting frame structure. (Simulation condition: g = 9.81 m/s^2, simulation time: 2 s in the y-direction and 16 s in the z-direction).

that the PDVA decreases the displacement of the vibrating structure at the target frequency value. Note that the y-axis of the FRF graph is presented in the form of ln for clearer visualization of changes in FRF values. In addition, the time-displacement graph also shows the decrease in displacement in the time domain, revealing that the existence of PDVA affects the target node response. As the simple finite element simulation shows the validity of the PDVA in efficiently suppressing vibrations, the study aims to determine the optimal locations of PDVAs in structures to enhance their efficiencies.

2. Optimization formulation

This section presents the optimization formulations for the GA and Voronoi diagram concept. The real coded GA (RCGA) was implemented in MATLAB to solve the optimization problem by formulating the optimized configuration of PDVAs. The integer design variables, indicating the node numbers of finite element models, were set as the design variables, and the locations of PDVAs were set as the nodes of the lattice and plane structures. The Voronoi diagram is implemented to uniformly distribute the PDVAs by dividing the structure into sub-domains.

2.1 Real coded genetic algorithm

A GA constitutes a family of heuristic and stochastic optimization methods. Based on the principle of survival of the fittest, a GA simulates the biological evolution process using a computer software to help determine a better individual or solution. In the GA theory, the diversity and convergence (domination of particular solutions) of the population matter. From an evolutionary perspective, the selection and crossover operations make the offspring inherit the parent characteristics imprinted on chromosomes. In contrast, the mutation operator introduces new characteristics to chromosomes. After sufficient generations, new better individuals can be introduced by the selection process, considering fitness values formulated by the optimization problem of interest. The implementation of these processes has been applied to various scientific and engineering problems. Compared with a gradient-based optimizer, the primary advantages of a GA is that they generate multiple solutions and individuals spread through the solution space, and thus, it has a higher chance of determining the global optimum. As a population is typically employed in GAs, it is also one of the advantages that a set of solutions close to the global optimum can be obtained through the population. In addition, GAs only use the objective function or fitness value. Compared to the gradient-based optimizer assuming the continuity of the first or second derivatives and function values, GAs can be applied to optimization problems whose derivatives are not available or continuities are not guaranteed.

The flowchart in Figure 3 shows a basic GA. First, random initial populations are generated; their genotypes and phenotypes each represent the locations of nodes and solutions of the problem, respectively. An RCGA, implemented in MATLAB, was used for encoding integer design variables. The fitness values are an integration of the frequency responses of structures with PDVAs, which were evaluated in the process. The frequency response functions were obtained by solving the nonlinear transient FEA to consider the coupling of pendulum and spring-mass motions. After obtaining the frequency response functions, parents were selected by considering the fitness values of individuals. Subsequently, the crossover and mutation operators were applied. The offspring replacement was conducted for the new generation and population, with an elitism in which the best individuals of the current population were maintained in the next generation. The probabilities of the crossover and mutation were set as the default values in the GA. The diversity of population in the GA is lost with larger possibilities.

The genotype of design variables represents the location of PDVAs. The encoding of GAs was performed using the RCGA. The crossover and mutation operators are the mixed integer-Laplace crossover power mutation algorithm. Larger population sizes increase the chances of finding the global optimum. However, as the nonlinear transient FEA simulation requires a considerable computation time, an

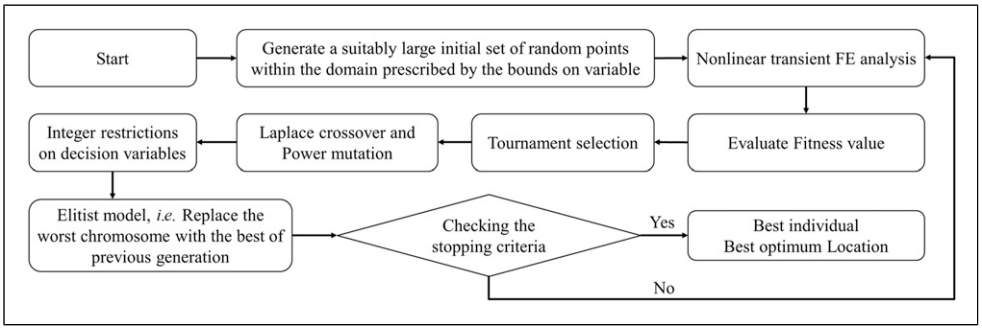

Figure 3. Optimization procedure based on the GA for an optimal PDVA structure.

auxiliary database of individuals and their fitness values are built to reduce the computation time. Moreover, when the phenotype of a new offspring is found in a database, individuals and their fitness values are saved and used without the finite element procedure.

2.2 Optimization formulation and encoding

To identify the optimal locations of PDVAs, the structural optimization problem is formulated with the frequency response functions of the displacements, that is, d_x, d_y, and d_z, as follows

$$\begin{aligned} &\underset{\mathbf{x}}{\text{Min}} f(\mathbf{x}) = \sum_{f=1}^{NF} \int_{\Omega_{start}^{i}}^{\Omega_{end}^{i}} x(\omega)d\omega + y(\omega)d\omega + z(\omega)d\omega \\ &\mathbf{x} = [x_1, x_2, \ldots, x_i],\ 1 \le x_i \le \mathrm{N} \end{aligned} \tag{10}$$

The objective function f is set as the integration value of the frequency responses from Ω_{start}^{i} to Ω_{end}^{i}. The frequency domain of interest is denoted by NF. Displacement of the nodes of interest are denoted by $x(\omega)$, $y(\omega)$, and $z(\omega)$. The optimization formulation can be reformulated without loss of generality. Based on the optimization formulation, $\mathbf{x}$ denotes the i number of integer design variables, and N denotes the number of finite element nodes.

2.3 Domain decomposition by the Voronoi diagram

The concept of Voronoi diagram was used to realize a uniform distribution of PDVAs within a hosting structure. The Voronoi diagram is a partition of a plane into regions close to each of a provided set of objects. The Voronoi diagram was applied considering lattice and plane structures to divide a structure into several sub-domains. Then, the geometry information (coordinates of x and y) of the divided sub-domains are obtained and used to identify the structural nodes included in the sub-domains. The mapping approach of the integer design variables was adopted to locate PDVAs at each sub-domain of a structure by adjusting the nodal numbers. Figure 4 presents the application of the Voronoi diagram and mapping approach on a simple lattice structure.

A simple lattice structure with 16 nodes is divided into four sub-domains, each with four nodes. The mapping approach changes the integer values of the number of nodes. For instance, the node with an initial node number of 8 changes to node 4 within the second sub-domain. This approach is efficient in detecting the locations of PDVAs at each sub-domain when more complicated structures with many sub-domains are explored. Therefore, the uniform distribution of PDVAs can be realized by using the division of structures obtained from the Voronoi diagram scheme and mapping approach and by limiting the number of PDVAs that can be installed in each sub-domain. Several case studies using these methods are presented in the next section.

3. Numerical problems

To demonstrate the validity of the proposed PDVA optimization, several optimization problems were explored to determine the optimized locations of PDVAs within vibrating structures. Nonlinear transient FEA simulations were performed in the framework of ANSYS. Transient displacement responses at the target nodes were then post-processed for their frequency response functions, which were required for the optimization formulation.

3.1 Optimal location of a PDVA structure at an inclined structure

For the first illustrative numerical example, the optimization is considered with one PDVA and one design variable, as shown in Figure 5(a). A straight structure with a length of 4 m comprises 100 frame elements with an inclination angle of 45°. The structure was set to have a Young's modulus of 193 GPa, Poisson's ratio of 0.31, and density of 7750 kg/m^3. The cross-sectional area of the frame was 0.1 m by 0.05 m. A mass of 10 kg was attached, and an impact force of 1000 N was applied in the x-direction at the end of the frame structure. In this optimization problem, a single PDVA with a mass of 10 kg, length of 0.0608 m, and spring constant of

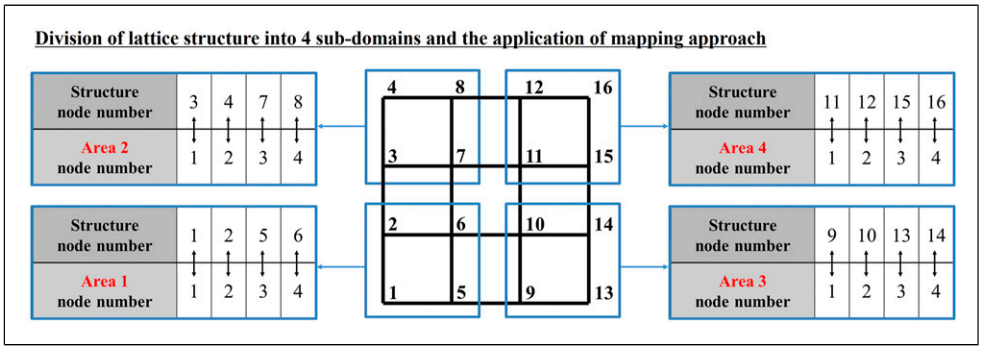

Figure 4. Application of the Voronoi diagram and mapping approach on lattice structures.

7.260×10^4 N/m was attached to one of the nodes of the hosting structure. The hosting frame structure is affected by both the pendulum and spring-mass motions. The pendulum and spring-mass resonance frequencies were 2.042 and 13.56 Hz, respectively. Thus, the optimization problem could be formulated to maximize the vibration reduction of the target node (node 50) at the two resonance frequencies by optimizing the location of PDVA. The particular optimization problem with one design variable for one PDVA structure can be set as follows

$$\begin{aligned} &\underset{\mathbf{x}}{\text{Min}} f(\mathbf{x}) = \int_{1.8}^{2.2} y(\omega)d\omega + \int_{13.2}^{13.8} y(\omega)d\omega \\ &y(\omega): \text{Displacement of node 50 in the y} - \text{direction} \\ &\mathbf{x} = [x_1],\ 1 \le x_i \le 100 \end{aligned} \tag{11}$$

where f denotes the objective function and $\mathbf{x}$ denotes the integer design variable. $y(\omega)$ denotes the frequency response function in the y-direction of the 50th node (target node). The population size, maximum generation number, and employed crossover fraction were set as 5, 50, and 0.8, respectively. The other variables were set as default values in MATLAB. The design variable, which denotes the node number where the PDVA is installed, is set to vary from 1 to 100.

The optimization history of the best and mean fitness values are shown in Figure 5(b). Some oscillations are observed for the mean fitness value curve owing to the diversity of the proposed GA. The best fitness value of 3.5465×10^{-3} m/Ns was obtained at the 46th iteration, and the 73rd node was found to be the optimum nodal position for the PDVA. As Elitism was applied to the replacement operator, the best individual is maintained during the evolution. Figure 6 presents a comparison of the frequency responses with and without the attached PDVA at the 73rd node, and the transient displacement at the target node with and without the PDVA. The results show that the frequency responses are reduced by 88.1674% and 34.6622% at 2.042 Hz and 13.56 Hz, respectively. Using the optimized PDVA structure, the oscillations in the structure can be reduced at the target frequencies. The responses at the two resonance frequencies were suppressed only with the proposed PDVA structure. Unlike other vibration absorbers, this absorber reduced the vibration at two frequency values. Moreover, the target frequencies can be altered by changing the values of the mass, spring constant, and length of the PDVA.

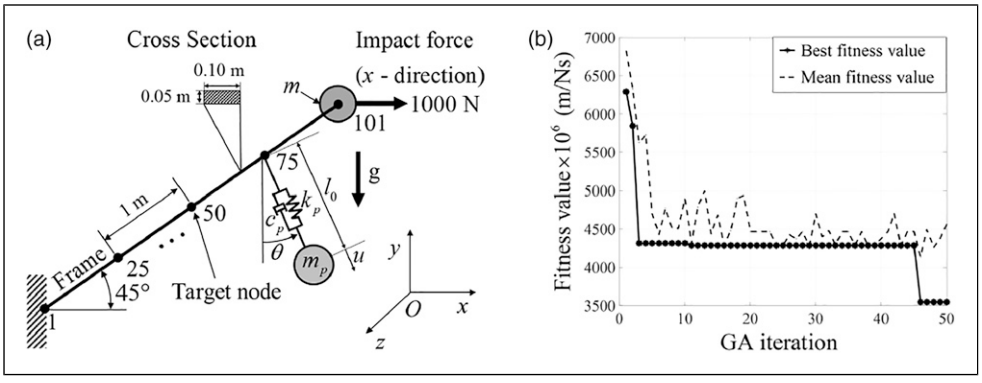

Figure 5. Optimization of the PDVA location: (a) Finite element model of the PDVA attached to the frame structure (Simulation condition: g = 9.81 m/s^2, simulation time: 16 s) and (b) the optimization history.

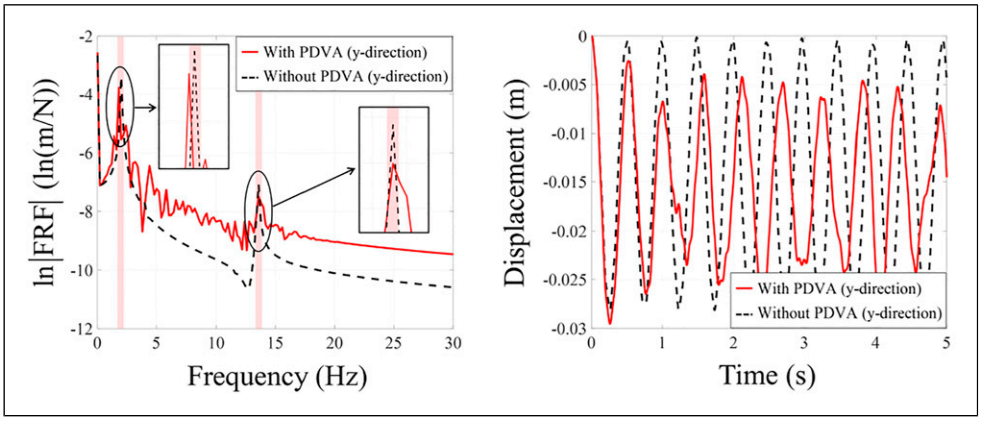

Figure 6. Responses of the target node (50th node) at the optimum design.

3.2 Optimal location of three PDVA structures at 10×20 grid lattice structure

In the next example, the optimization process aims to determine the optimum locations of the three PDVAs. Figure 7(a) illustrates the problem definition. A lattice frame structure with a length of 1 m and height of 2 m consisted of 200 elements. The lattice structure was set to have a Young's modulus of 193 GPa, Poisson's ratio of 0.31, and density of 7750 kg/m^3. The cross-section area of the frame was 0.01 m by 0.01 m. A mass of 5 kg was attached to the top right of the structure. Impact forces of 10 N were applied in the y- and z-direction at node 91. In this example, three PDVAs with different parameters were considered. The mass of all the three PDVAs was 2 kg; their lengths were 0.1974 m, 0.0180 m, and 0.1974 m; and their spring constants were 101.3 N/m, 1.109 × 10^3 N/m, and 3.899 × 10^4 N/m. The frequencies of the PDVAs were set considering the first three resonance frequencies of the grid lattice structure. The calculated spring-mass and pendulum resonance frequencies of the first PDVA had equal values of 1.133 Hz. The calculated spring-mass and pendulum resonance frequencies of the second PDVA had equal values of 3.748 Hz. The calculated spring-mass and pendulum resonance frequencies of the third PDVA were 22.22 and 1.133 Hz, respectively. The optimization formulation for this example can be set as follows

$$\begin{aligned} \underset{\mathbf{x}}{\text{Min}} f(\mathbf{x}) &= \int_{0.8}^{1.4} z(\omega)d\omega + \int_{3.4}^{4.0} z(\omega)d\omega \\ &\quad + \int_{22.0}^{22.8} y(\omega)d\omega \\ y(\omega) &: \text{Displacement of node 231} \quad \text{in the y} - \text{direction} \\ z(\omega) &: \text{Displacement of node 231} \quad \text{in the z} - \text{direction} \\ \mathbf{x} &= [x_1, x_2, x_3],\ 1 \le x_i \le 231 \end{aligned} \tag{12}$$

where f denotes the objective function and $\mathbf{x}$ denotes the integer design variables. $y(\omega)$ and $z(\omega)$ represent the frequency response functions in the y- and z-direction of the 231st node (target node), respectively. The population size, maximum generation number, and employed crossover fraction were set as 20, 50, and 0.8, respectively. In addition, the design variables, which denote the node numbers where the PDVAs are installed, were set to vary from 1 to 231.

As the design variables are integers, the GA can be applied to solve the optimization formulation in equation (12). The total number of finite element nodes was 231, and the GA was applied with 20 initial populations. The optimization history of the best and mean fitness values are shown in Figure 7(b). The best fitness value of 4.3109 × 10^{-4} m/Ns was obtained at the 18th iteration, and the optimum nodal positions for the three PDVAs were obtained. The optimum nodal positions of the three PDVAs are the 23rd, 207th, and 105th nodes of the structure, as illustrated in Figure 8. The results show that the frequency responses are reduced by 98.6549%, 84.4969%, and 65.4271% at 1.133 Hz, 3.748 Hz, and 22.22 Hz, respectively. Note that the y-direction frequency response is reduced at 22.22 Hz, and the z-direction frequency responses are reduced at 1.133 Hz and 3.748 Hz, as desired. The results indicate that the optimized PDVAs successfully suppress the structural vibrations of desired directions at desired frequencies.

3.3 Optimal location of six PDVA structures using the Voronoi diagram

In the next optimization problem, the optimum locations of the six PDVAs were determined in the subdivided design domain, as shown in Figure 9(a). The L-shaped lattice structure consists of 75 elements with Young's modulus, Poisson's ratio, and density of 193 GPa, 0.3, and 7750 kg/m^3, respectively. The cross-section area of the lattice structure was set to 0.01 m by 0.01 m. Impact forces of 100 N were applied in the y- and z-direction at the bottom right of the structure. As the mass, length, and spring constant were set to 0.5 kg, 0.2857 m, and 96.12 N/m,

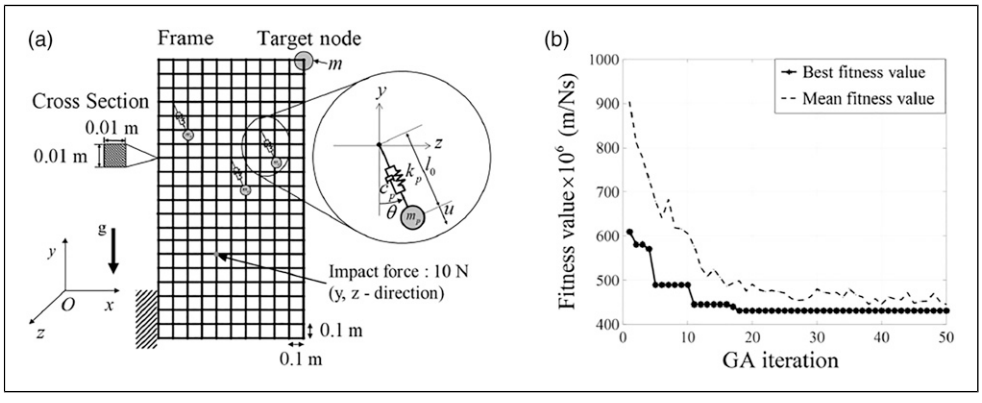

Figure 7. Optimization of the three PDVA locations: (a) Finite element model of the PDVAs attached to the lattice frame structure (Simulation condition: g = 9.81 m/s^2, simulation time: 5 s) and (b) optimization history.

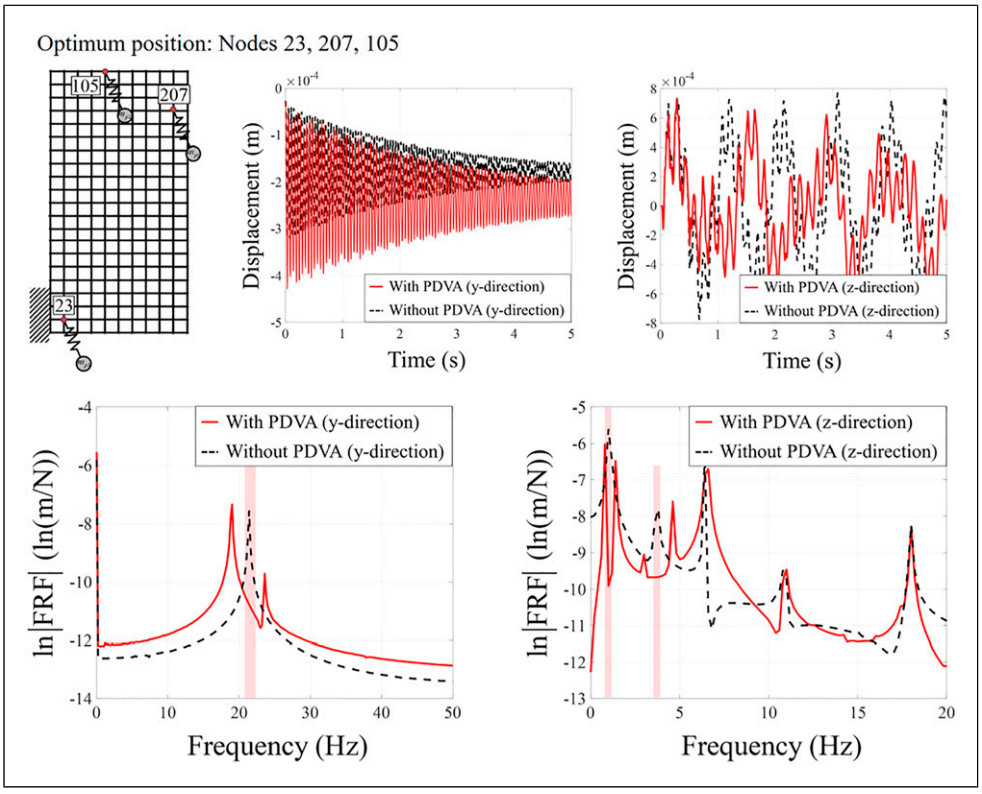

Figure 8. Optimum positions of the three PDVAs and responses of the target node (231st node) at the optimum design.

respectively, the resonance frequency values of the pendulum and spring-mass systems were set to 0.9417 and 2.2027 Hz, respectively. Considering these resonance frequencies, the optimization formulation for this example can be set as follows

$$\begin{aligned} &\underset{\mathbf{x}}{\text{Min}} f(\mathbf{x}) = \int_{0.8}^{1.0} z(\omega)d\omega + \int_{1.8}^{2.8} y(\omega)d\omega \\ &y(\omega): \text{Displacement of node 96 in the y} - \text{direction} \\ &z(\omega): \text{Displacement of node 96 in the z} - \text{direction} \\ &\mathbf{x} = [x_1, x_2, x_3, x_4, x_5, x_6],\ 1 \le x_i \le 96 \end{aligned} \tag{13}$$

where f denotes the objective function and $\mathbf{x}$ denote the integer design variables. The frequency response functions in the y- and z-direction of the 96th node (target node) are denoted by $y(\omega)$ and $z(\omega)$, respectively. The population size, maximum generation number, and employed crossover fraction were set as 10, 50, and 0.8, respectively. The design variables, which denote the node numbers where the PDVAs were installed, were set to vary from 1 to 96.

This example was aimed to realize a uniform distribution of the PDVAs within the hosting L-shaped structure. For instance, PDVA structures can be installed on buildings; however, the installation can be often irritating to residents. A uniform distribution of PDVAs is one of the solutions. To distribute the PDVAs uniformly, the hosting structure can be divided into sub-domains, and a design constraint can be imposed to install limited number of PDVAs in a single sub-domain. To this end, we proposed to apply the Voronoi diagram to divide the L-shaped structure into sub-domains. For example, an application of the Voronoi diagram scheme to divide a design domain is shown in Figure 10. In this example, the L-shaped design domain was divided into six sub-domains, and the mapping approach of the integer design variables was implemented to locate the PDVAs for each sub-domain by adjusting the nodal numbers. For instance, area 1 divided by the Voronoi diagram consists of 9 nodes, and each nodes are given new nodal numbers from 1 to 9. To perform the optimization in this particular example, it was assumed that only one PDVA can be installed in each sub-domain.

The GA was again applied to solve equation (13) while considering the sub-domains divided using the Voronoi diagram scheme. The GA was solved using ten initial populations. The optimization history of the best and mean fitness values are shown in Figure 9(b). The best fitness value of 1.4552×10^{-2} m/Ns was obtained at the sixth iteration, and the optimal nodal positions for the six PDVAs were obtained. Figure 10 illustrates the optimum nodal positions. The 5th, 3rd, 7th, 1st, and 8th nodes from areas 1 to 6 were found to be the optimal nodal positions at each divided sub-domain, indicating that nodes 3, 11, 30, 41, 42, and 92 of the host structure are the optimal positions

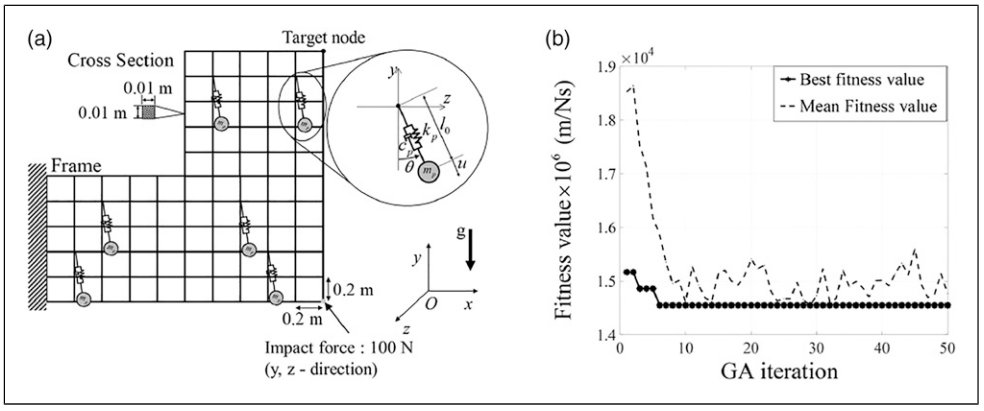

Figure 9. Optimization of the six PDVA locations: (a) Finite element model of the PDVAs attached to the lattice structure (Simulation condition: g = 9.81 m/s^2, simulation time: 10 s) and (b) the optimization history.

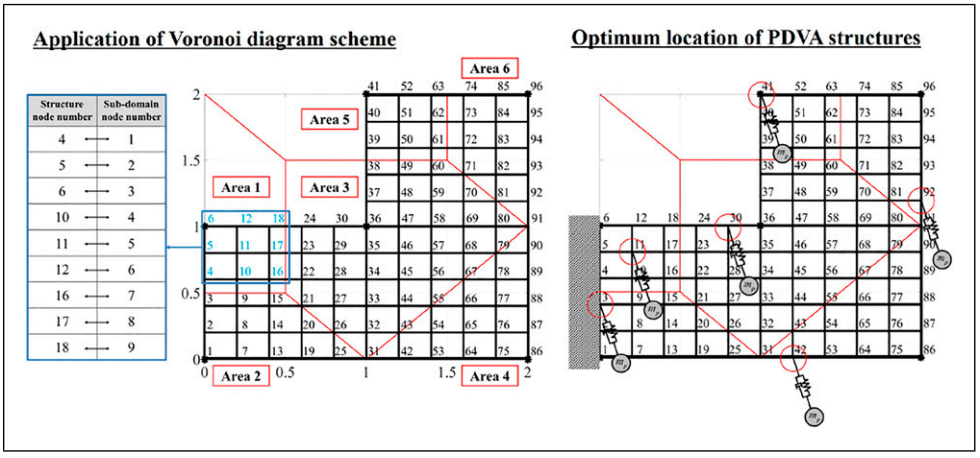

Figure 10. Application of the Voronoi diagram and optimization results of the L-shape structure.

for the six PDVAs. Figure 11 illustrates the frequency response functions and transient responses of the optimized structure. The results show that the frequency responses are reduced by 74.3175% and 37.1236% at 0.9417 Hz and 2.2027 Hz, respectively. Note that the y-direction frequency response is reduced at 2.2027 Hz, and the z-direction frequency response is reduced at 0.9417 Hz, as desired. The results indicate that the optimized PDVAs successfully suppress the structural vibrations of desired directions at desired frequencies. This example also reveals that the Voronoi diagram scheme can be used for the application of PDVAs. The proposed optimization approach helps the installation of PDVAs to attenuate the vibrations.

3.4 Optimal location of eleven PDVA structures using the Voronoi diagram

In the final example, the optimization problem was aimed to determine the optimum locations of eleven PDVAs. The problem definition is presented in Figure 12(a). An L-shaped plane structure with a void consisted of 295 plane elements. The Young's modulus, Poisson's ratio, and the density were set to 193 GPa, 0.31, and 7750 kg/m^3, respectively. Impact forces of 200 N were applied in the x- and y-direction at the top right of the structure. In this example, the PDVAs had a point mass of 0.3 kg, length of 1.967×10^{-2} m, and spring constants of 4.907×10^3 N/m. Thus, the resonance frequencies of the pendulum and spring-mass systems were 3.5883 and 20.3560 Hz, respectively. The optimization formulation for the example can be set as follows

$$\begin{aligned} &\min_{\mathbf{x}} f(\mathbf{x}) = \int_{3.0}^{4.0} y(\omega)d\omega + \int_{18.8}^{20.8} y(\omega)d\omega \\ &y(\omega): \text{Displacement of node 22 in the y} - \text{direction} \\ &\mathbf{x} = [x_1, x_2, x_3, \ldots, x_{11}],\ 1 \le x_i \le 981 \end{aligned} \tag{14}$$

where the objective function is denoted by f and the integer design variables are denoted by $\mathbf{x}$. The frequency response

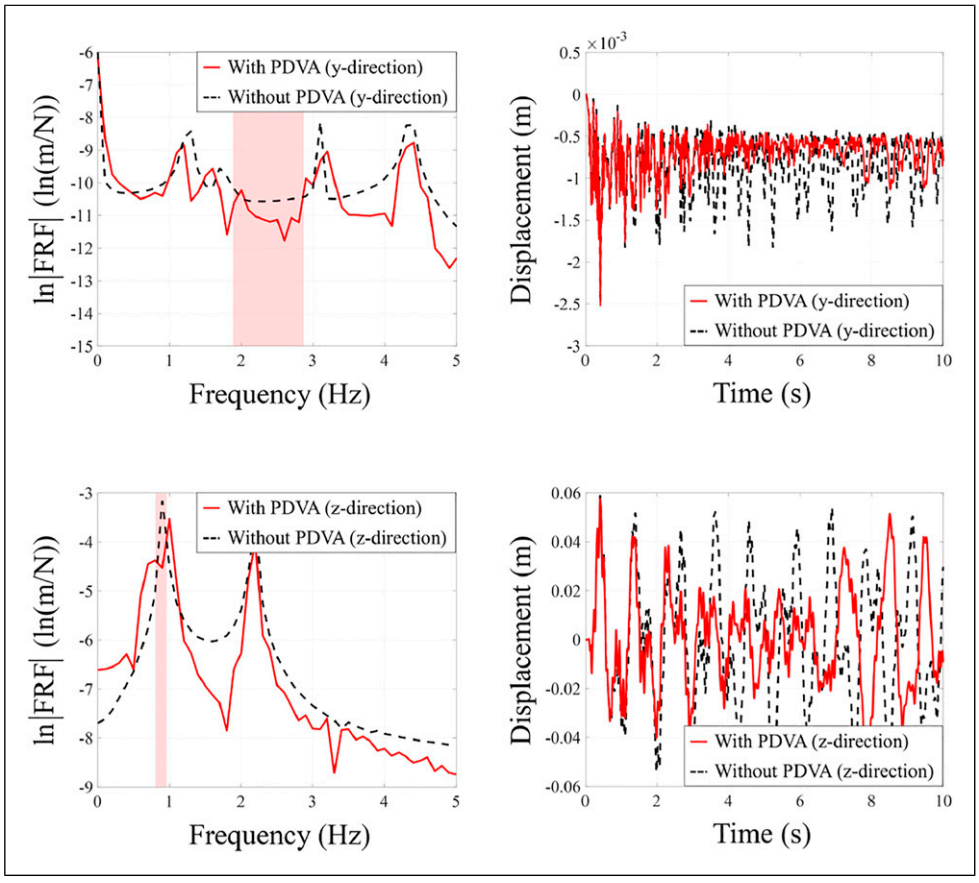

Figure 11. Responses of the target node with optimized layouts: (a) y-direction and (b) z-direction.

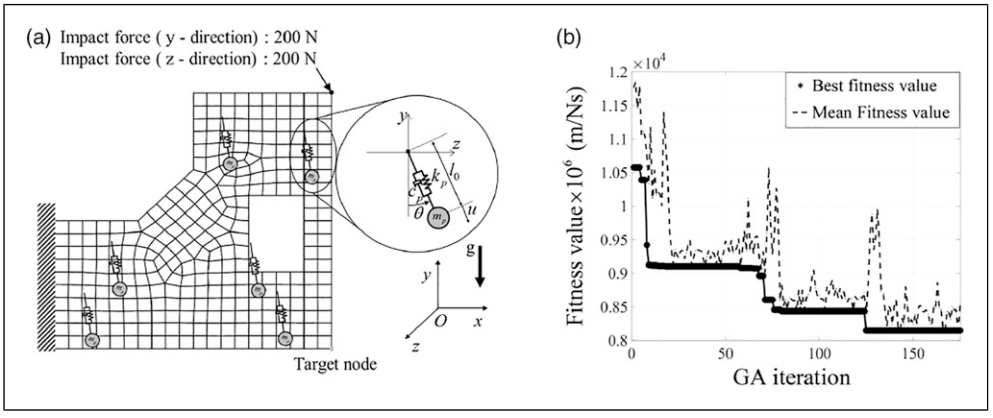

Figure 12. Optimization of eleven PDVA locations: (a) Finite element model of the PDVAs attached to the plane structure with void (Simulation condition: g = 9.81 m/s^2, simulation time: 5 s) and (b) the optimization history.

function in the y-direction of the 22nd node (target node) is denoted by $y(\omega)$. The population size, maximum generation number, and employed crossover fraction were set as 10, 50, and 0.8, respectively. The design variables, which denote the node number where the PDVAs are installed, were set to vary from 1 to 981.

Similar to the previous example, this example was aimed to realize a uniform distribution of PDVAs. The concept of Voronoi diagram was used to divide the hosting structure into sub-domains. The application of the Voronoi diagram is shown in Figure 13. It was assumed that the design domain can be divided into 11 sub-domains, and only one PDVA

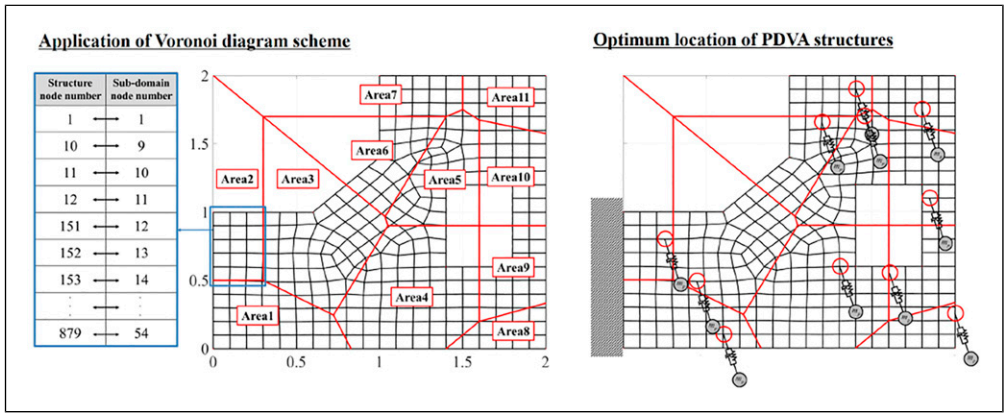

Figure 13. Application of the Voronoi diagram and optimization results of the L-shape structure with void.

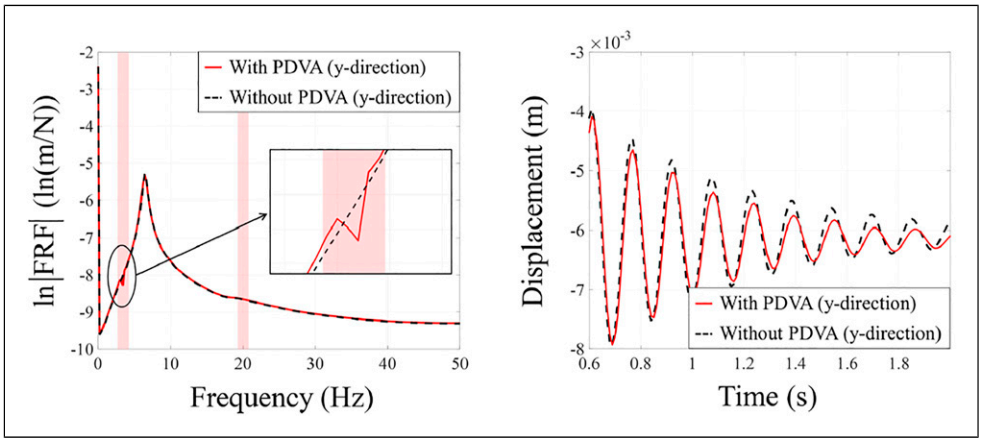

Figure 14. Responses of the target node with optimized layouts.

could be installed in each sub-domain. The mapping approach of integer design variables to locate the PDVAs was implemented.

A GA was applied to solve equation (14) while considering the sub-domains divided using the Voronoi diagram scheme. The total number of element nodes was 981, and the GA was solved using ten initial populations. The optimization history of the best and mean fitness values are shown in Figure 12(b). The best fitness value of 8.1421×10^{-3} m/Ns was obtained at the 122nd iteration, and the optimal nodal positions for the 11 PDVAs were obtained. The optimum nodal positions are shown in Figure 13. The 100th, 38th, 78th, 152nd, 27th, 29th, 47th, 18th, 43rd, 31st, and 46th nodes from areas 1 to 11 were found to be the optimal nodal positions at each divided sub-domain, indicating that nodes 757, 474, 691, 828, 544, 449, 793, 67, 371, 292, and 469 of the host structure are the optimal positions for the eleven PDVAs. The frequency response function and transient response of the optimized structure are shown in Figure 14. The results show that the frequency responses are reduced by 20.9895% and 0.7541% at 3.5853 Hz and 20.3560 Hz, respectively. This example shows that the Voronoi diagram scheme can be used for more complicated problems considering PDVAs. With the proposed optimization approach, the installation of PDVAs can suppress the vibrations.

The optimization problems presented in this section proved that GA can determine the optimum locations of PDVAs. The resonance frequencies of the pendulum and spring-mass systems of PDVAs were tuned independently by varying the pendulum mass, spring constant, and pendulum length for effective vibration suppression of the hosting structures. Moreover, the concept of Voronoi diagrams and a mapping approach were applied to distribute PDVAs uniformly within the lattice and plane structures. The installation of PDVAs is effective regardless of the geometry of the hosting structure and element type, indicating that the proposed optimization method can be applied to real-life engineering problems with a capability to solve structural instabilities.

4. Conclusions

We presented an optimum design for structures with PDVAs using a GA. Achieving structural stability through vibration

suppression is a critical issue in the engineering field. To overcome this issue, PDVAs were utilized to attenuate vibrations using the resonances of the pendulum and spring-mass systems. A GA was used to determine the optimal locations of PDVAs in the hosting structures. We considered the installation of PDVAs on the finite element nodes and junctions of lattice structures to validate the proposed method. The optimization formulations helped to determine optimal structural designs with vibrations suppressed at the desired resonant frequencies. In the proposed optimization method, we applied the Voronoi diagram to divide hosting structures into sub-domains and realize a uniform distribution of PDVAs. The numerical examples presented in the paper demonstrated the effectiveness of PDVAs in suppressing structural vibrations, where frequency responses were reduced by maximum of 98.6549% at desired frequency values. Despite the structural complexity, the present PDVA successfully suppresses the structural vibrations of desired directions at target frequencies. In conclusion, this study presents and validates the optimization method to determine optimal locations of PDVAs in various structures. As future work, the present method can be expanded by applying different optimization techniques. It will be valuable to compare the efficiencies of different discrete optimization algorithms for the optimization of the PDVA locations and enhancement in vibration attenuation. Additionally, through experimental verification and validation, the findings of the present paper can be verified for various structures and the difficulties in the application of PDVA in real life should be exploited.

Declaration of conflicting interests

The author(s) declared no potential conflicts of interest with respect to the research, authorship, and/or publication of this article.

Funding

The author(s) disclosed receipt of the following financial support for the research, authorship, and/or publication of this article: This work was supported by the National Research Foundation of Korea (NRF) grant funded by the Korean government (MSIT) (NRF-2019R1A2C2084974 and 2017R1A3B1023591).

ORCID iD

Gil Ho Yoon https://orcid.org/0000-0002-0634-8329

References

Abdelkareem MA, Xu L, Ali MKA, et al. (2018) Vibration energy harvesting in automotive suspension system: a detailed review. *Applied Energy* 229: 672699.

Aykan M and Celik M (2009) Vibration fatigue analysis and multiaxial effect in testing of aerospace structures. *Mechanical Systems and Signal Processing* 23(3): 897907.

Besseghier A, Houari MSA, Tounsi A, et al. (2017) Free vibration analysis of embedded nanosize fg plates using a new nonlocal trigonometric shear deformation theory. *Smart Structures System* 19(6): 601614.

Chapain S and Aly AM (2019) Vibration attenuation in high-rise buildings to achieve system-level performance under multiple hazards. *Engineering Structures* 197: 109352.

Chopard B and Tomassini M (2018) Particle swarm optimization. In: *An Introduction to Metaheuristics for Optimization*. Cham, Switzerland: Springer, 97102.

Chuangwen X, Jianming D, Yuzhen C, et al. (2018) The relationships between cutting parameters, tool wear, cutting force and vibration. *Advances in Mechanical Engineering* 10(1): 1687814017750434.

Couceiro M and Ghamisi P (2016) Particle swarm optimization. In: *Fractional Order Darwinian Particle Swarm Optimization*. Cham, Switzerland: Springer, 110.

Das S, Mandal A and Mukherjee R (2013) An adaptive differential evolution algorithm for global optimization in dynamic environments. *IEEE Transactions on Cybernetics* 44(6): 966–978.

Dong X, Lian J, Wang H, et al. (2018) Structural vibration monitoring and operational modal analysis of offshore wind turbine structure. *Ocean Engineering* 150: 280297.

Ebrahimi F, Barati MR and Civalek O (2020) Application of chebyshev–ritz method for static stability and vibration analysis of nonlocal microstructure-dependent nanostructures. *Engineering with Computers* 36(3): 953964.

Elmadih W, Chronopoulos D, Syam WP, et al. (2019) Three-dimensional resonating metamaterials for low-frequency vibration attenuation. *Scientific Reports* 9(1): 11503.

Galvan B, Greiner D, Periaux J, et al. (2003) Parallel evolutionary computation for solving complex cfd optimization problems: A review and some nozzle applications. in Matsuno K, Ecer A, Satofuka N, Periaux J, Fox P, (Eds.) *Parallel Computational Fluid Dynamics 2002* Amsterdam, North-Holland: 573604.

Ghayesh MH (2018) Nonlinear vibration analysis of axially functionally graded shear-deformable tapered beams. *Applied Mathematical Modelling* 59: 583596.

Gürgen S and Sofuolu MA (2020) Vibration attenuation of sandwich structures filled with shear thickening fluids. *Composites Part B: Engineering* 186: 107831.

Ha SI and Yoon GH (2021) Numerical and experimental studies of pendulum dynamic vibration absorber for structural vibration. *Journal of Vibration and Acoustics* 143(1): 011013.

Hamza-Cherif R, Meradjah M, Zidour M, et al. (2018) Vibration analysis of nano beam using differential transform method including thermal effect. *Journal of Nano Research* 54: 114.

He W, Wang T, He X, et al. (2020) Dynamical modeling and boundary vibration control of a rigid-flexible wing system. *IEEE/ASME Transactions on Mechatronics* 25(6): 27112721.

Hussain M, Naeem MN and Taj M (2019) Vibration characteristics of zigzag and chiral functionally graded material rotating carbon nanotubes sandwich with ring supports. *Proceedings of the Institution of Mechanical Engineers, Part C: Journal of Mechanical Engineering Science* 233(16): 57635780.

Jafarboland M and Farahabadi HB (2018) Optimum design of the stator parameters for noise and vibration reduction in bldc motor. *IET Electric Power Applications* 12(9): 12971305.

Jena PC (2018) Identification of crack in sic composite polymer beam using vibration signature. *Materials Today: Proceedings* 5(9): 1969319702.

Jiang L, Feng Y, Zhou W, et al. (2019) Vibration characteristic analysis of high-speed railway simply supported beam bridge-track structure system. *Steel and Composite Structures* 31(6): 591600.

Kachitvichyanukul V (2012) Comparison of three evolutionary algorithms: ga, pso, and de. *Industrial Engineering and Management Systems* 11(3): 215223.

Kaddari M, Kaci A, Bousahla AA, et al. (2020) A study on the structural behaviour of functionally graded porous plates on elastic foundation using a new quasi-3d model: bending and free vibration analysis. *Computers and Concrete* 25(1): 3757.

Kalehsar HE and Khodaie N (2018) Optimization of response of a dynamic vibration absorber forming part of the main system by the fixed-point theory. *KSCE Journal of Civil Engineering* 22(7): 2354–2361.

Krenk S (2005) Frequency analysis of the tuned mass damper. *Journal of Applied Mechanics* 72(6): 936–942.

Lai J, Tan T, Yang S, et al. (2021) Flow-induced vibration of tube bundles considering the effect of periodic fluid force in a rotated triangular tube array. *Annals of Nuclear Energy* 161: 108488.

Lu L, Guo X and Zhao J (2017) Size-dependent vibration analysis of nanobeams based on the nonlocal strain gradient theory. *International Journal of Engineering Science* 116: 1224.

Luo Y, Zhang Z, Zhang K, et al. (2021) Test evaluation on vibration reduction effect of compacted stone mastic asphalt mixture. *Journal of Materials in Civil Engineering* 33(5): 04021092.

Meng H, Chronopoulos D, Fabro AT, et al. (2020) Rainbow metamaterials for broadband multi-frequency vibration attenuation: Numerical analysis and experimental validation. *Journal of Sound and Vibration* 465: 115005.

Patnaik SS, Roy T and Rao DK (2021) Numerical investigation of vibration characteristics and damping properties of cnt-based viscoelastic spherical shell structure. In: *Vibration Engineering for a Sustainable Future*. Cham, Switzerland: Springer, 231238.

Phung-Van P, Thai CH, Nguyen-Xuan H, et al. (2019) An isogeometric approach of static and free vibration analyses for porous fg nanoplates. *European Journal of Mechanics - A/Solids* 78: 103851.

Pourjabari A, Hajilak ZE, Mohammadi A, et al. (2019) Effect of porosity on free and forced vibration characteristics of the gpl reinforcement composite nanostructures. *Computers & Mathematics with Applications* 77(10): 26082626.

Prawin J and Rama Mohan Rao A (2020) Vibration-based breathing crack identification using non-linear intermodulation components under noisy environment. *Structural Health Monitoring* 19(1): 86104.

Qin AK, Huang VL and Suganthan PN (2008) Differential evolution algorithm with strategy adaptation for global numerical optimization. *IEEE Transactions on Evolutionary Computation* 13(2): 398417.

Qin B, Zhong R, Wang T, et al. (2020) A unified fourier series solution for vibration analysis of fg-cntrc cylindrical, conical shells and annular plates with arbitrary boundary conditions. *Composite Structures* 232: 111549.

Saini MK, Bagha AK, Kumar S, et al. (2021) Finite element analysis for predicting the vibration characteristics of natural fiber reinforced epoxy composites. *Materials Today: Proceedings* 41: 223227.

Sheng M, Guo Z, Qin Q, et al. (2018) Vibration characteristics of a sandwich plate with viscoelastic periodic cores. *Composite Structures* 206: 5469.

Syam WP, Jianwei W, Zhao B, et al. (2018) Design and analysis of strut-based lattice structures for vibration isolation. *Precision Engineering* 52: 494506.

Wu Y, Qiu J, Zhou S, et al. (2018) A piezoelectric spring pendulum oscillator used for multi-directional and ultra-low frequency vibration energy harvesting. *Applied Energy* 231: 600614.

Yoon J, Ru C and Mioduchowski A (2005) Vibration and instability of carbon nanotubes conveying fluid. *Composites Science and Technology* 65(9): 13261336.

Zhang L, Wu Q, Ma Z, et al. (2019) Transient vibration analysis of unit-plant structure for hydropower station in sudden load increasing process. *Mechanical Systems and Signal Processing* 120: 486504.

Zhao C and Prasad MG (2019) Acoustic black holes in structural design for vibration and noise control. *Acoustics* 1: 220251.

Zhao L and Yang Y (2018) An impact-based broadband aeroelastic energy harvester for concurrent wind and base vibration energy harvesting. *Applied Energy* 212: 233243.

Zhao X, Ji C and Bi S (2021) Spatial correlation effect of a multidimensional force on vibration suppression. *Aerospace Science and Technology* 117: 106928.

Zou J, Lan H, Xu Y, et al. (2017) Analysis of global and local force harmonics and their effects on vibration in permanent magnet synchronous machines. *IEEE Transactions on Energy Conversion* 32(4): 15231532.